Characterization of α-Al_2O_3 coatings deposited by reactive evaporation in an anodic arc under high-current ion assistance

Characterization of α-Al_2O_3 coatings deposited by reactive evaporation in an anodic arc under high-current ion assistance

A S Kamenetskikh[1,2], N V Gavrilov[1], P V Tretnikov[1] and A V Chukin[2]

[1] Institute of Electrophysics UD RAS, 106 Amundsena Str., Yekaterinburg, 620016, Russia
[2] Ural Federal University, 19 Mira Str., Yekaterinburg, 620002, Russia

E-mail: alx@iep.uran.ru

Abstract. The article presents the results of studies of the mechanical and adhesive characteristics of α-Al_2O_3 coatings depositeedby reactive anodic evaporation of Al in an arc discharge at low-energy (50 eV) high-current (up to 15 mA·cm^{-2}) ion assistance at 640°C. The coatings are characterized by a strong texture (300), which contributes to an increase in adhesive strength (the critical load at which the destruction of the coating is observed reaches 2560±29 mN). It was shown that there is an optimal discharge current (20 A), at which the best adhesion, the surface quality (R_a = 13.4 nm, R_z = 44.7 nm) and the resistance of elastic deformation of coatings (H/E = 0.08) are achieved.

1. Introduction

Alumina in acrystalline state has high performance, while the amorphous phase is characterized by low heat resistance and hardness [1]. Coatings from the thermostable Al_2O_3 phase are used as protective coatings on cutting tools [2] and in friction pairs that heat up to temperatures over 800°C [3]. The ion nature of the chemical bond in Al_2O_3 allows maintaining the chemical stability of the oxide at high temperatures and, unlike metals, providing low adhesion with the contact surface. Due to this, Al_2O_3 coatings very effectively prevent abrasive wear of tools, but at the same time require additional adhesive layers on the substrate surface and have thickness limitations because of the decreasing adhesion of coatings due to the high level of intrinsic stresses. The technology of deposition of α-Al_2O_3 coatings should provide low-temperature (600°C and below) crystallization of coatings [4–6] at high-speed deposition (more than 1 μm·h^{-1}) [7, 8] and reduction of intrinsic stresses in coatings in order to increase their adhesive strength. The comprehensive solution to these tasks is complicated by the mutually exclusive nature of conditions required to achieve the result. For example, the high migratory mobility of adatoms, which is necessary for the formation of nanocrystalline coatings at low temperatures, is achieved through an increase in the intensity of bombardment of the coating surface with ions with energies of 100–200 eV during its growth [8–11]. This leads, firstly, to growing intrinsic stresses in coatings and the deterioration of their adhesion [12], and secondly, to the reduction of the crystallite size [13] to values, at which the α-phase cannot be stabilized [14]. At the high-rate deposition of α-Al_2O_3 coatings, there is a need for an appropriate increase in intensity of ion assistance in order to maintain the required level of energy per atom in the coating [5].

This paper examines the microstructure and properties of α-Al_2O_3 coatings obtained by reactive anode evaporation in an arc at the substrate temperature of 640°C. The used concept of high-rate deposition of nanocrystalline coatings with low intrinsic stresses is based on the previous results [15, 16]. High-current (current density up to 15 mA·cm^{-2}) low-energy (~ 50 eV) ion assistance has been used; conditions for the increased concentration of atomic oxygen in plasma and reduced ionisation of metal vapour have been created. This work was aimed at finding optimal discharge modes and coating deposition conditions that allow achieving high mechanical and adhesive properties of α-Al_2O_3 coatings.

2. Experimental methods

The coatings were deposited in a gas discharge system with a self-heated hollow cathode, a thermo-isolated anode-crucible (further crucible) and an additional hollow anode. The outer surface of the hollow anode was covered with a ceramic screen; the aperture area was 1 cm^2. A detailed description of the device is provided in [13]. Ar and O_2 have been supplied separately to the discharge gap through the cathode and hollow anode, respectively. The partial pressure of Ar was 0.13 Pa; the pressure of O_2 was adjusted in the range of 0–0.26 Pa through changing the gas flow within 50–150 sccm.

The currents on the crucible and hollow anode were adjusted separately. The maximum current of crucible was 4 A, the temperature of the crucible reached 1050°C, and the pressure of the metal vapour was ~ 10^{-3} Torr. The density of the ion current on the sample surface was adjusted within 4–15 mA·cm^{-2} through changing of hollow anode current in the range of 4–36 A. The imposition of the O_2 flow and a larger part of electronic discharge current in a small aperture of the hollow anode provided a significant increase in the degree of gas dissociation, which was confirmed by the results of plasma discharge optical spectroscopy [17].

The coatings were deposited to AISI430 steel samples with sizes of 15×15×1 mm^3. A 100 nm thick layer of chromia, which is isostructural to α-Al_2O_3, was preliminarily formed on the sample surface by reactive magnetron sputtering. Samples were heated by a radiation heater up to 640°C. The negative potential of the samples was set in a pulse mode (50 kHz, 10 μs) with an amplitude of 50 V.

The thickness of the coatings was determined by the ball-cratering method using a Calotest device (CSM Instruments) with 0.1 μm accuracy. The hardness of the coatings and the Young modulus were measured using an ultramicrohardness tester DUH-211/211S (Shimadzu) by the Oliver-Pharr method [18]. At least 20 measurements were taken for each sample at the penetration depth of no more than 10% of coating thickness. The indentor load and unloading curves were analyzed in order to determine the work of the indentor at elastic and plastic deformation of the coating [19].

X-ray analysis of coatings was carried out using an x-ray diffractometer XRD-7000 (Shimadzu) in Cu-Kα radiation with a graphite monochromator on the secondary beam. The recording was performed in the diffraction angle range of 15–107° by 2θ, with a scan step 0.05° and the time of one step 5 s. The decryption of XRD-patterns was done using the XPert High Score Plus software and PDF-2 databases. The size of the crystallites and the magnitude of the microdistortions were determined by the true physical expansion of diffraction lines according to the Williamson-Hall method using reference sample data and Rietveld full-profile analysis.

The level of intrinsic stresses in the coatings was assessed using the ratio [20]: $\sigma = E/2\mu\Delta d/d$, where E is the Young modulus, μ –the Poisson coefficient, $\Delta d/d$ – microstrain of the crystal lattice. The calculation results did not take into account the influence of factors such as the distribution of local stress fields near grain boundaries and were used only for qualitative evaluation.

The adhesion strength of the coatings was determined using scratching with a conical diamond indentor Rockwell C (rounding radius 5 μm) on a Nanotest 600 device. Accurate determination of the critical indentor load, which leads to the breaking of the coating, required an analysis of the indentation depth, the response of acoustic emission and the image of scratches. Up to 5 scratches were applied to the sample surface in two stages: in the first stage, the indentor was moving along the sample surface at a distance of 500 μm with a speed of 5 μm·s^{-1} at a constant normal load of 0.1 mN. At this load level and in the absence of significant surface deformation, the roughness parameters R_a

(average surface roughness) and R_z (maximal surface roughness) of have been measured. In the second stage, the indentor was moving along the sample surface at a distance of 1000 μm with a speed of 5 m·s^{-1} and a load that was linearly increasing with a speed of 20 mN·s^{-1}. The critical load L_{cr}, at which the coating chipped off from the substrate, was recorded by the acoustic response.

The structure of the coatings in the cross-section of samples obtained through the cleavage technique was examinedusing an electron microscope LEO 982 (LEO Electronenmikroskopie GmbH, Germany).

3. Results

The XRD analysis of coatings deposited at abias voltage of 50 V in the range of hollow anode currents 4–36 A has shown that α-Al_2O_3 is the main phase. The most intense reflexes of this phase correspond to 2θ ~ 25.7° (012), 37.9° (110), 52.8° (024), 68.5° (300) (figure 1). Crystallites have a predominant orientation (300) with the Harris texture coefficient [6] reaching 6. The average size of α-Al_2O_3 coherent scattering regionis monotonously reduced from ~ 140 to 82 nm when anode current increases up to 36 A. Increasing the O_2 flow up to 150 sccm also contributes to the reduction of sizes of crystallites down to 65 nm. A detailed analysis reveals the γ-phase of Al_2O_3 in the coatings obtained at anode currents less than 20 A. Low intensity of reflexes and large line width do not allow accurate estimation of the volume content of γ-Al_2O_3.

Figure 2 shows the dependences of coating hardness and the ratio of hardness to the Young modulus H/E on the anode current. Hardness varies from 18 to 24 GPa; the maximum value is reached at the current 20 A. The Young modulus varies in the range of 260–330 GPa. The value of H/E also changes non-monotonicallyand reaches the maximum value ~ 0.079 at the anode current 16–20 A. For comparison, one can specify that the solidity of the sapphire monocrystal is 28 GPa and the Young modulus is 409–441 GPa, respectively [1].

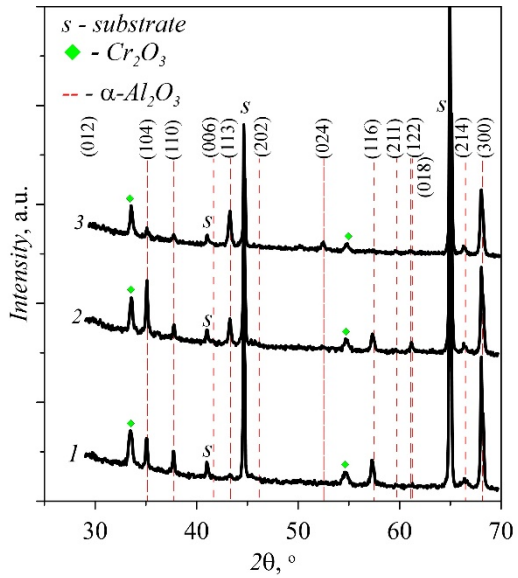

Figure 1. XRD spectra of Al_2O_3 coatings. Anode current: *1* – 4 A; *2* – 20 A; *3* – 36 A.

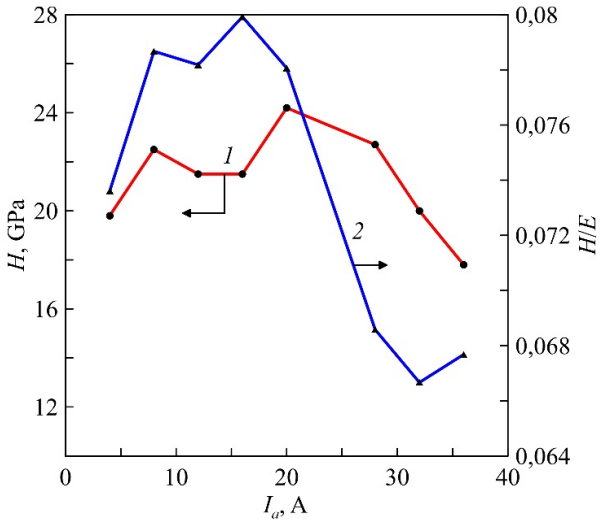

Figure 2. Dependences of hardness (*1*) and the ratio of hardness to the Young modulus of the coating on the anode current.

It is known that high values of H/E (~ 0.1) indicate good wear resistance of coatings at sliding friction and elastic deformation, especially under static loads [22]. However, high H/E is not enough for good wear resistance of the coating under the conditions of the dominating adhesive mechanism of destruction and intensive deformation of the surface layer. The ability of the coating to dissipate deformation energy becomes very important [23].

The microhardness dissipation parameter MDP is determined from the relationship of energies consumed by the indentor at elastic (W_e) and plastic (W_p) deformation of the coating: MDP = 1 $-W_e/(W_e + W_p)$ [23]. The dependence of MDP on the anode current is shown in figure 3. With an increase in current up to 20 A, MDP reaches the minimal value of 0.37 and then monotonously increases up to 0.44 at the current 36 A. The MDP values of the obtained coatings are below the values for monocrystalline α-Al_2O_3 (0.55) [24] and are comparable with values for nanocomposite [25] and multi-component $(Al,Cr)_2O_3$ coatings [26]. The MDP and hardness of the coatings in the anode current function (figure 2) correlate with the magnitude of intrinsic stresses in the coatings, the maximum value of which was 1.8 GPa (figure 3).

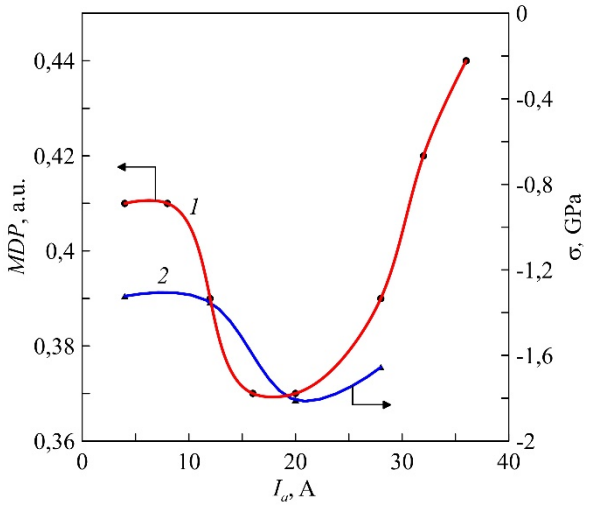

Figure 3. Dependences of MDP (*1*) and intrinsic stresses (*2*) of coating on the anode current.

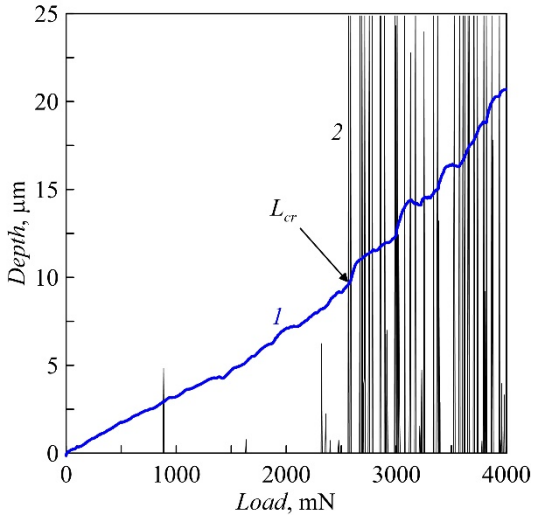

Figure 4. Dependence of the scratch depth (*1*) on the normal load and acoustic emission signal (*2*).

The results of measuring the adhesion strength of the coatings and roughness of their surface are presented in table 1. Acoustic emission peaks and the dependence of indentation depth on load are shown in figure 4. The maximal strength of adhesion (L_{cr} = 2560 mN) is achieved at the anode current 20 A; a further increase in current leads to a decrease in L_{cr} of the coating.

Table 1. The critical load L_{cr} and the parameters of surface roughness of the coatings.

Anode current (A)	L_{cr} (mN)	R_a (nm)	R_z (nm)
4	1912 ± 41	22.8 ± 1.6	101.3 ± 6.8
12	2031 ± 60	36.9 ± 7	123.8 ± 24.7
20	2560 ± 23	13.4 ± 0.6	44.7 ± 4
28	1445 ± 29	227.1 ± 18.9	767.1 ± 10.9

Average surface roughness R_a is 13–23 nm, with the lowest values being reached at the current 20 A (table 1). Coatings with minimal values of R_a and R_z were obtained at the anode current 20 A. A further increase in the current results in a dramatic increase in the roughness of the coating surface.

Figure 5 shows images of a cross-section of the coatings obtained by the cleavage technique and their surface. It is evident that at the anode current up to 20 A, smooth coatings are formed. An increase in current up to 28 A is accompanied by recrystallization of individual grains with their tops

reaching the surface and then increasing of their linear sizes. Such grains are formed both directly in the surface layer of the coating and at a depth of more than 1 μm.

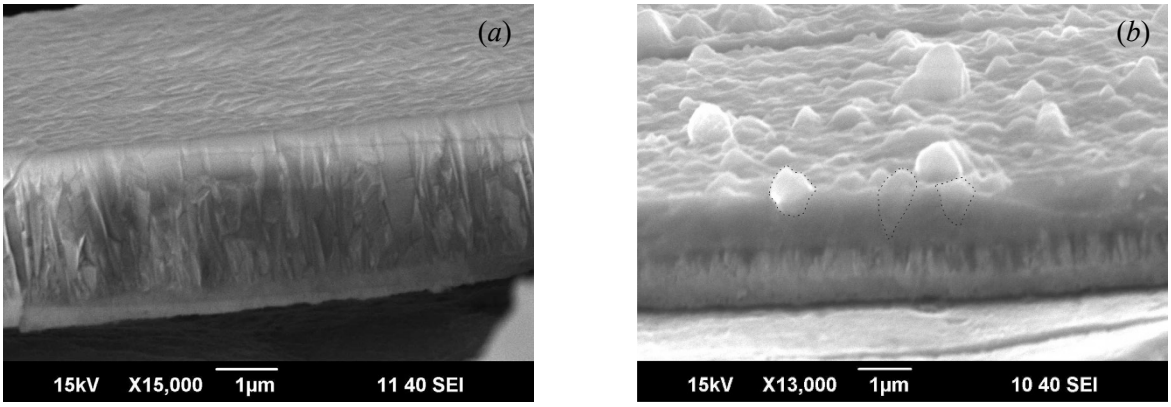

Figure 5. SEM images of the cross-section of Al_2O_3 coating. Anode current: *a* – 20 A; *b* – 28 A.

4. Discussion

According to the Davis model [27], the growth of compression stresses in crystalline coatings occurs in a certain range of energies of ions that bombard the growing surface of the coating. Thermal peaks that occur when energy increases above this range, on the contrary, deactivate crystal lattice defects and reduce intrinsic stresses. The energy of ions, at which maximal compression stresses in coatings of different compositions are reached, isabout 100 eV [28]. In the coatings depositedat low-energy (50 eV) high-current (up to 15 $mA \cdot cm^{-2}$) ion assistance, the stress level does not exceed 1.8 GPa. Since stresses induced in the low-energy range are proportional to the energy of ions as 2/3 [28], then an increase in energy up to 100 eV would lead to the growth of stresses up to ~ 2.9 GPa, which is consistent with the results of the previous experiments [13].

Lower levels of intrinsic stresses are typical for amorphous (10 MPa) [29] and amorphous-crystalline γ-Al_2O_3 coatings (0.5–1 GPa) with thickness up to 1.2 μm [30], with the hardness of such coatings not exceeding 6.3 and 15 GPa, respectively, and MDP being equal to ~ 0.35. When the proportion of the crystalline γ-Al_2O_3 phase in such coatings increases, the stress level grows up to 3 GPa; increasing the bias voltage of the sample up to 150 V does not lead to the formation of the α-Al_2O_3 phase and is accompanied by the growth of intrinsic stresses up to 10 GPa. In the work [31], thick (4–6 μm) single-phase α-Al_2O_3 coatings were obtained at the floating potential of the substrates and a temperature of no less than 700°C. The level of intrinsic stresses in such coatings reached 20 GPa.

A low level of intrinsic stresses in the coatings obtained in this work is provided by limiting the energy of the gas ions on the coating surface at 50 eV. The formation of the α-phase at a low temperature and ion energy is achieved by an increase in the current density of gas ions and the degree of O_2 dissociation. It has been shown in the previous work [13] that at a given amount of ion energy there is a minimum density of ion current, exceeding which allows forming single-phase α-Al_2O_3 coatings. An increase in the proportion of oxygen atoms in the reactive gas flow on the coating surface leads to a reduction in energy costs for dissociation (496 $kJ \cdot mol^{-1}$), the magnitude of which is comparable to the activation energy of α-Al_2O_3 formation (589 $kJ \cdot mol^{-1}$ for amorphous→α and 526 $kJ \cdot mol^{-1}$ for γ→α transitions) [32]. The adhesion strength of the resulting coatings is an order of magnitude greater than the strength of the amorphous Al_2O_3 coatings of a comparable thickness (L_{cr} = 278 mN [33], 16 mN [34]) and nanocrystalline γ-Al_2O_3 coatings (170 mN) [35].

Another feature of coatings obtained by reactive thermal anode evaporation is the presence of strong preferential orientation of crystallites. It has been shown in the works [24, 36] that the main deformation mechanism for α-Al_2O_3 is a basal slip. The resulting dislocations are characterized by Burgers vectors $b = 1/3\{10\bar{1}0\}$ (b = 0.274 nm) and $b = 1/3\{11\bar{2}0\}$ (b = 0.475 nm) and slide plane

(001). The obtained α-Al_2O_3 coatings have strong texture, and the crystals has preferential orientation (300) perpendicular to the direction of development of dislocations. This feature of the structure helps to increase the resistance of coatings to plastic deformation. The decrease in the texturing of coatings is accompanied by a decrease in *H/E* down to ~ 0.063–0.068, corresponding to monocrystalline samples obtained under equilibrium conditions [1].

According to the experimental results, α-Al_2O_3 coatings with the highest *H/E* (~ 0.08) deposited at the anode current 20 A are also characterized by the greatest adhesion strength (L_{cr} = 2560 mN). Anincrease in the anode current accompanied by a decrease in the coefficient of texture (300) also leads to a sharp decrease in *H/E* and adhesion strength of coatings. One can conclude that the *H/E* parameter is related to the adhesion strength of α-Al_2O_3 coatings and indicate that strong texture (300) is a favorable factor for achieving high mechanical and adhesion characteristics.

5. Conclusion

The mechanical and adhesive properties of α-Al_2O_3 coatings deposited by reactive anode evaporation in high-current discharge with a hollow anode at 640°C and bias voltage 50 V have been studied. The coatings are mainly characterized by the preferred orientation of crystallites (300), which enhances their mechanical and adhesive characteristics. The optimal discharge current for the best adhesion (L_{cr} = 2560±23 mN) and resistance to elastic deformation of coatings (*H*/*E* = 0.08) was 20 A. Coatings deposited in the optimal mode are characterized by a high quality of the surface (R_a = 13.4 nm, R_z = 44.7 nm). Elevated discharge current values (28–36 A) provide the formation of coatings that are close to monocrystalline α-Al_2O_3 in their structural-phase state and mechanical characteristics and possess high values of the microhardness dissipation parameter (0.44). However, theroughness (R_a = 227 nm, R_z = 767 nm) and adhesive strength (L_{cr} = 1445 ± 29 mN) of such coatings have significantly deteriorated. The low level of intrinsic stresses (1.8 GPa) provides the increased adhesion strength of the resulting α-Al_2O_3 coatings up to 10 μm thick, the value of which is an order of magnitude greater than that of coatings deposited by alternative methods.

Acknowledgments

This work was supported by the Russian Science Foundation under grant No. 18-19-00567.

References

[1] Levin I and Brandon D 1998 *J. Am. Ceram. Soc.* **81** 1995
[2] Bobzin K 2017 *CIRP Journal of Manufacturing Science and Technology* **18** 1
[3] Lux B, Colombier C and Altena H 1986 *Thin Solid Films* **138** 49
[4] Schneider J M, Sproul W D, Voevodin A A and Matthews A 1997 *J. Vac. Sci. Technol. A* **15** 1084
[5] Prenzel M, Kortmann A, Stein A, Keudell A, Nahif F and Schneider J M 2013 *J. Appl. Phys.* **114** 113301
[6] Jin P, Nakao S, Wang S X and Wang L M 2003 *Appl. Phys. Lett*. **82** 1024
[7] Lin Y, Wang C and Tao J 2013 Surf. Coat. Technol. **235** 544
[8] Sarakinos K, Music D, Nahif F, Jiang K, Braun A, Zilkens C and Schneider J M 2010 *Phys. Status Solidi RRL* **4** 154
[9] Wallin E, Selinder T I, Elfwing M and Helmersson U 2008 EPL **82** 36002
[10] Rosen J, Mraz S, Kreissig U, Music D and Schneider J M 2005 *Plasma Chemistry and Plasma Processing* **25** 303
[11] Brill R, Koch F, Mazurelle J, Levchuk D, Balden M, Yamada-Takamura Y, Maier H and Bolt H 2003 *Surf. Coatings Technol*. **174-175** 606
[12] Li Q, Yu Y-H, Bhatia C S, Marks L D, Lee S C and Chung Y W 2000 *J. Vac. Sci. Technol. A* **18** 2333
[13] Gavrilov N V, Kamenetskikh A S, Tretnikov P V and Chukin A V 2018 *Surf. Coatings Technol.* **337** 453

[14] McHale J M, Auroux A, Perrotta A J and Navrotsky A 1997 *Science* **277** 788
[15] Gavrilov N V, Kamenetskikh A S, Trernikov P V, Emlin D R, Chukin A V and Surkov Yu S 2019 *Surf. Coatings Technol.* **359** 117
[16] Gavrilov N V, Kamenetskikh A S, Emlin D R, Tretnikov P V and Chukin A V 2019 *Technical Physics* **64(6)** 807
[17] Kamenetskikh A S, Gavrilov N V, Solomonov V I, Surkov Yu S, Ershov A A and Tretnikov P V 2018 *Journal of Physics: Conf. Series* **1115** 032073
[18] Oliver W C and Pharr G M 1992 *J. Mater. Res.***7** 1564-83
[19] Milman Yu V, Galanov B A and Chugunova S I 1993 *Acta Metall. Mater.* **41** 2523
[20] Noyan I C and Cohen J B 1987 *Residual Stress. Measurement by Diffraction and Interpolation* (Springer-Velgar, New York)
[21] Harris G B 1952 *Philos. Mag. Series 7* **43** 113
[22] Musil J 2012 *Surf. Coat. Technol.* **207** 50
[23] Fox-Rabinovich G S, Veldhuis S C, Scvortsov V N, Shuster L Sh, Dosbaeva G K and Migranov M S 2004 *Thin Solid Films* **469–470** 505
[24] Engelhart W, Dreher W, Eibl O and Schier V 2011 *Acta Materialia* **59** 7757
[25] Ferre F G, Bertarelli E, Chiodoni A, Carnelli D, Gastaldi D, Vena P, Beghi M G and Fonzo F D 2013 *Acta Materialia* **61** 2662
[26] Bobzin K, Brцgelmann T, Kalscheuer C and Welters M 2018 *Thin Solid Films* **663** 131
[27] Davis C A 1993 *Thin Solid Films* **226** 30
[28] Bilek M M M and McKenzie D R 2006 *Surf. Coat. Technol*. **200** 4345
[29] Morgner H, Neumann M, Straach S and Krug M 1998 *Surf. Coat. Technol*. **108–109** 513
[30] Musil J, Blazek J, Zeman P, Proksov S, Sasek M and Cerstvy R 2010 *Appl. Surf. Sci*. 257 1058
[31] Zywitzki O, Hoetzsch G, Fietzke F and Goedicke K 1996 *Surf. Coat. Technol.* **82** 169
[32] Zeman P, Zuzjakova S, Blazek J, Cerstvy R and Musil J 2014 *Surf. Coat. Technol.* **240** 7
[33] Nath S, Manna I, Ray S K and Majumdar J D 2016 *Ceramics International* **42** 7060
[34] He X D, Dong L, Wu J and Li D 2019 *J Surf. Coat. Technol.* **365** 65
[35] Khanna A, Bhat D G, Harris A and Beake B D 2006 *Surf. Coat. Technol.* **201** 1109
[36] Heuer A H, Lagerlof K P D and Castaing 1998 *J. Philos. Mag.***78** 747